

**A COMPARATIVE STUDY OF LUNG CANCER DETECTION USING DEEP
TRANSFER LEARNING WITH KERAS TUNER**

BY

**Sajeeb Datta
ID: 201-15-3119**

This Report Presented in Partial Fulfillment of the Requirements for the Degree of
Bachelor of Science in Computer Science and Engineering

Supervised By

Ms. Lamia Rukhsara
Lecturer (Senior Scale)
Department of CSE
Daffodil International University

Co-Supervised By

Md. Sabab Zulfiker
Senior Lecturer
Department of CSE
Daffodil International University



DAFFODIL INTERNATIONAL UNIVERSITY

DHAKA, BANGLADESH

JANUARY 2024

APPROVAL

This Project titled "A COMPARATIVE STUDY OF LUNG CANCER DETECTION USING DEEP TRANSFER LEARNING WITH KERAS TUNER", submitted by Sajceb Datta, ID No: 201-15-3119 to the Department of Computer Science and Engineering, Daffodil International University has been accepted as satisfactory for the partial fulfilment of the requirements for the degree of B.Sc. in Computer Science and Engineering and approved as to its style and contents. The presentation has been held on 26-01-2024

BOARD OF EXAMINERS



Dr. Md. Taimur Ahad (MTA)
Associate Professor & Associate Head
Department of Computer Science and Engineering
Daffodil International University

Chairman



Abdus Sattar(AS)
Assistant Professor
Department of Computer Science and Engineering
Daffodil International University

Internal Examiner



Tapasy Rabeya(TRA)
Senior Lecturer
Department of Computer Science and Engineering
Daffodil International University

Internal Examiner



Dr. Md. Zulfiker Mahmud (ZM)
Associate Professor
Department of Computer Science and Engineering
Jagannath University

External Examiner

DECLARATION

We hereby declare that this project has been done by us under the supervision of **Ms. Lamia Rukhsara, Lecturer (Senior Scale), Department of CSE Daffodil International University**. We also declare that neither this project nor any part of this project has been submitted elsewhere for the award of any degree or diploma.

Supervised by:

Lamia Rukhsara
Ms. Lamia Rukhsara
Lecturer (Senior Scale)
Department of CSE
Daffodil International University

Co-Supervised by:

For
Lamia Rukhsara
Md. Sabab Zulfiker
Senior Lecturer
Department of CSE
Daffodil International University

Submitted by:

Sajeed Datta
Sajeed Datta
ID: 201-15-3119
Department of CSE
Daffodil International University

ACKNOWLEDGEMENT

First, we express our heartiest thanks and gratefulness to almighty God for His divine blessing made us possible to complete the final year project/internship successfully.

We really grateful and wish our profound indebtedness to **Supervisor Ms. Lamia Rukhsara, Lecturer (Senior Scale)**, Department of CSE, Daffodil International University, Dhaka. Deep Knowledge & keen interest of our supervisor in the field of “**Deep Convolutional Neural Networks**” to carry out this project. Her endless patience, scholarly guidance, continual encouragement, constant and energetic supervision, constructive criticism, valuable advice, reading many inferior drafts and correcting them at all stages have made it possible to complete this project.

We would like to express our heartiest gratitude to **Ms. Lamia Rukhsara** and **Dr. Sheak Rashed Haider Noori** Head, Department of CSE, for their kind help to finish our project and also to other faculty members and the staff of the CSE department of Daffodil International University.

We would like to thank our entire coursemates at Daffodil International University, who took part in this discussion while completing the coursework.

Finally, we must acknowledge with due respect the constant support and patients of our parents.

Abstract

Lung cancer is a type of cancer that begins in the cells of the lungs. It is one of the most common forms of cancer worldwide and is a leading cause of cancer-related deaths. Lung cancer usually develops in the cells lining the air passages of the lungs. There are two main types of lung cancer: non-small cell lung cancer (NSCLC) and small cell lung cancer (SCLC). NSCLC is the most prevalent, comprising about 85% of all lung cancer cases, while SCLC is generally more aggressive and tends to spread quickly. The need for early detection is underscored by the fact that lung cancer symptoms often manifest at advanced stages, limiting treatment options and reducing the likelihood of successful intervention. This thesis presents a comprehensive study on the application of six pre-trained convolutional neural network models, namely MobileNetV2, InceptionV3, ResNet50, VGG16, VGG19, and NASHNetMobile, for the classification of lung cancer categories. The dataset used in this research consists of 15,000 images, spanning three distinct classes: Lung Adenocarcinoma, Lung Benign Tissue, and Lung Squamous Cell Carcinoma. To optimize model performance, hyperparameter tuning is employed using the Keras Tuner framework. This approach allows for the systematic exploration of hyperparameter configurations to enhance the models' accuracy and generalization. The hyperparameters include learning rates, dropout rates, and other key parameters crucial for model training. The results indicate that MobileNetV2 achieved the highest accuracy among the tested models, with an impressive 98.47%. Following closely, VGG16 demonstrated the second-best performance, achieving an accuracy of 98.40%. The study contributes valuable insights into the practical application of deep learning models for medical image classification tasks, particularly in the context of lung cancer diagnosis. The reported accuracies demonstrate the potential of leveraging pre-trained models to enhance the efficiency and accuracy of computer-aided diagnostic systems for early detection of lung cancer.

TABLE OF CONTENTS

CONTENTS	PAGE
Board of examiners	i
Declaration	ii
Acknowledgement	iii
Abstract	iv
List of Figures	vii
List of Tables	ix
CHAPTER	
CHAPTER 1: INTRODUCTION	1-3
1.1 Introduction	1
1.2 Motivation	1
1.3 Rationale of the Study	2
1.4 Research Questions	2
1.5 Expected Output	2
1.6 Project Management and Finance	2
1.7 Report Layout	3
CHAPTER 2: BACKGROUND STUDY	4-8
2.1 Preliminaries	4
2.2 Related Works	4
2.3 Comparative Analysis and Summary	8
2.4 Scope of the Problem	8
2.5 Challenges	8

CHAPTER 3: METHODOLOGY	9-20
3.1 Research Subject and Instrumentation	9
3.2 Data Collection Procedure/Dataset Utilized	9
3.3 Statistical Analysis	10
3.4 Proposed Methodology/Applied Mechanism	19
3.5 Implementation Requirements	20
CHAPTER 4: EXPERIMENTAL ANALYSIS & RESULTS	21-31
4.1 Environment Setup	21
4.2 Experimental Result and Analysis	21
4.3 Discussion	31
CHAPTER 5: IMPACT ON SOCIETY, ENVIRONMENT & SUSTAINABILITY	32
5.1 Impact On Society	32
5.2 Impact On Environment	32
5.3 Ethical Aspects	32
5.4 Sustainability Plan	32
CHAPTER 6: SUMMARY, CONCLUSION, RECOMMENDATION AND IMPLICATION FOR FUTURE RESEARCH	33-34
6.1 Summary of the Study	33
6.2 Conclusion	33
6.3 Implication for Further Study	33
REFERENCES	35-36

LIST OF FIGURES

FIGURES	PAGE NO
Figure 3.2: Sample Data	9
Figure 3.3.2: Transfer Learning Architecture	11
Figure 3.3.3: Convolutional Layer	12
Figure 3.3.4: Pooling Layer	12
Figure 3.3.5: Fully Connected Layer	13
Figure 3.3.6.1: Architecture of MobileNetV2	14
Figure 3.3.6.2: MobileNetV2 with Customize Layers	14
Figure 3.3.6.3: Architecture of ResNet50	15
Figure 3.3.6.4: Architecture of InceptionV3	16
Figure 3.3.6.5: Architecture of VGG16	16
Figure 3.3.6.6: Architecture of VGG19	16
Figure 3.3.6.7: Architecture of NASHNetMobile	17
Figure 3.3.7: Workflow of Keras	18
Figure 3.4: Workflow of the Proposed Methodology	19
Figure 4.2.1 MobileNetV2 Training-Validation Loss and Accuracy	22
Figure 4.2.2 Confusion Matrix of MobileNetV2	23
Figure 4.2.3 ResNet50 Training-Validation Loss and Accuracy	24
Figure 4.2.4 Confusion Matrix of ResNet50	24

Figure 4.2.5 InceptionV3 Training-Validation Loss and Accuracy	25
Figure 4.2.6 Confusion Matrix of InceptionV3	26
Figure 4.2.7 VGG-16 Training-Validation Loss and Accuracy	27
Figure 4.2.8 Confusion Matrix of VGG-16	27
Figure 4.2.9 VGG19 Training-Validation Loss and Accuracy	28
Figure 4.2.10 Confusion Matrix of VGG19	29
Figure 4.2.11 NASHNetMobile Training-Validation Loss and Accuracy	30
Figure 4.2.12 Confusion Matrix of NASHNetMobile	30

LIST OF TABLES

TABLES	PAGE NO
Table 2.3: Comparison Between Other Studies	8
Table 3.2: Data Description	9
Table 4.2.1: Comparison of This Study	21
Table 4.2.2: Classification Report of MobileNetV2	23
Table 4.2.3: Classification Report of ResNet50	25
Table 4.2.4: Classification Report of InceptionV3	26
Table 4.2.5: Classification Report of VGG16	28
Table 4.2.6: Classification Report of VGG19	29
Table 4.2.7: Classification Report of NASHNetMobile	31

CHAPTER 1

INTRODUCTION

1.1 Introduction

Lung cancer typically originates in the cells lining the airways of the lungs, posing an elevated risk of mortality for both men and women, and ranking as the primary cause of cancer-related death [5]. It can be broadly classified into two types: small cell (SCLC) and non-small cell (NSCLC), each requiring distinct cultivation and care approaches. NSCLC is more prevalent, accounting for the majority of lung cancer cases, making it the deadliest form with a 5-year survival rate below 20%. Early detection significantly improves the prognosis, leading to over 70% survival. NSCLC is further divided into squamous cell carcinoma (SCC) and adenocarcinoma (ADC). Computed tomography (CT) scans, producing three-dimensional chest images, are highly effective for detecting lung nodules [5]. Classic symptoms include fatigue, wheezing, chest pain, coughing up blood, weight loss, and shortness of breath. The elderly, particularly those aged 65 and older, are more susceptible, with lung cancer being the most common cancer globally and responsible for a quarter of all cancer-related deaths annually. Fortunately, fewer people are starting to smoke, contributing to a decline in new lung cancer cases. In 2020, an estimated 2.2 million new cases are expected globally, with varying rates in different regions, and the reliance on Deep Learning (DL) is justified due to its continuous accuracy improvement with increasing data.

1.2 Motivation

For detecting lung nodules, Histopathological images, the most efficient approach involves generating two-dimensional (2D) images of the lung using machines that produce three-dimensional images. However, it is not specific to any lung-related disease. This study can work with chest histopathological images for three categories of lung cancer (lung adenocarcinoma, lung squamous cell carcinoma and lung benign tissue) and successfully classify them with great accuracy. Further issues related to the detection of lung cancer, these models are capable of doing it and can be used in a variety of devices. Detection such as automatically identifying the disease without the assistance of a human. This will be less money and time consuming, and the process is easier, which will be beneficial for the medical sector.

1.3 Rationale of the Study

Most of the studies have dealt with low accuracy and fine-tuning issues detecting lung cancer. Some studies work with various technique to improve their accuracy, and many have gained low accuracy because of not tuning the model's parameter in the best way. So in this study, We have tried to find a way for fine-tuning the model that takes less human effort and low time. Thus, We have used Keras Tuner for tuning the model.

1.4 Research Questions

- How is the dataset collected?
- How many categories are in this dataset?
- How this dataset is preprocessed?
- How this work helps the medical sector?
- How this research will benefit the common people?

1.5 Expected Output

This research is based on Lung Cancer Detection. Here the categories of lung cancer are in three types: lung adenocarcinoma, lung squamous cell carcinoma and lung benign tissue. Here we tried to create an excellent deep transfer learning technique with some pre-trained algorithms by adding keras tuner for hyper parameter tuning that can detect the category of lung cancer. Here we have used five transfer learning algorithms to do this work.

1.6 Project Management and Finance

The research addresses risk management by employing six pre-trained models. Data management involves preprocessing techniques for images collected from online sources. The study's implementation on Jupyter Notebook utilizes six freely available pre-trained models, benefiting patients by automating the detection of lung diseases from histopathological images without extensive human assistance.

1.6.1 Risk Management

For doing this research there are some risk factors to lookout. Ensuring the best possible result we have employed six different pre-trained models. Every models accuracy and classification report has been provided. We also compare our research result with other researches that we have studied for this task.

1.6.2 Data Management

As the data were collected from online sources, we have applied some preprocessing techniques including resizing of the image, normalizing pixel values for getting the best result withing a short period of time.

1.6.3 Finance

The implementation of this study has been done on jupyter notebook. Six pre-trained models has been used for this disease detection task and these models were free to use as we have used them for extracting feature from the image.

In short, it is beneficial for patients who want to know about lung disease, because this process does not required more human help. This proposed model of ours automatically detect the category of lung disease from the given histopathological image of lung.

1.7 Report Layout

The remainder of the report is structured as follows:

Chapter 2 provides an overview of the study's Background, Chapter 3 outlines the Methodology employed in the study, Chapter 4 delves into the Experimental Results and Discussion, Chapter 5 explores the study's Impact on Society, Environment, and Sustainability, Chapter 6 encapsulates the Summary, Conclusion, Recommendation, and Implications for Future Research, and lastly, the References section.

CHAPTER 2

BACKGROUND STUDY

2.1 Preliminaries

Early Detection of Lung Cancer is a significant work for research to detect the category of the cancer. Lots of work are already have done in this topic using deep learning technique. Many information has been discovered through the research.

2.2 Related Works

Many academics have studied the identification of different diseases using data from lung histopathological image over the years. Furthermore, their efforts are not without restrictions. In the "background study" part, we will discover the methodologies used by the researchers, the quantity of lung histopathological image they used, the diagnoses they worked on, the models they used, and their accomplishments. This makes it evident how much they have improved and how flawed they still remain.

Guo et al. employed 3D Deep Learning and Radiomics techniques to achieve histological subtype classification of lung cancers based on CT images. They developed two fully automatic classification models, namely The ProNet and comradNet, to differentiate between the three subtypes of lung cancer using unenhanced CT scans. The authors reported an Area Under the Curve (AUC) of 84% for identifying the three groups, while ProNet demonstrated a 71% accuracy in the classification process[1].

Al-Huseiny.M.S. et al. utilized GoogLeNet transfer learning for the detection of lung cancer. The study comprehensively addressed aspects such as pre-processing, feature extraction, segmentation, and classification within the context of computerized medical data analysis. The authors employed genetic algorithms to identify optimal attributes for a support vector machine (SVM) based algorithm. The results of their research revealed a 93% accuracy using the SVM algorithm, while employing neural networks led to an increased accuracy of 95.87%. Additionally, the authors successfully predicted mortality rates with an accuracy of 96%[2].

Cai, Z. et al. explored Ensemble-based feature selection and machine learning techniques for the classification of lung cancer, aiming to discern the specific type and severity of the detected lung cancers. The study employed machine learning algorithms, specifically Random Forests (RFs) and Multi-Support Vector Machines (Multi-SVMs). Classification and regression tasks were conducted using RFs, achieving a notable accuracy of 86.54%, with a high recall accuracy of 85.5% through the Leave-one-out cross-validation (LOOCV) technique. The authors suggested that employing superior datasets and high-resolution images could further enhance the accuracy of their approach[3].

Radhika, P. R. et al. conducted a study employing machine learning algorithms to evaluate various approaches for detecting lung cancer. The primary focus of this research was to assess the efficacy of classification algorithms in facilitating early diagnosis of lung cancer. To predict lung cancer, the study utilized Naive Bayes, Decision Tree, Logistic Regression, and Support Vector Machine algorithms. Employing a supervised learning technique, the researchers constructed a model represented as a tree data structure through a decision tree. Remarkably, the model achieved the highest accuracy at 99.3%, indicating excellent performance in the context of early lung cancer diagnosis[4].

Althubiti, S. A. et al. presented a study on the early detection of lung cancer through CT image-based analysis, employing an ensemble learning system integrated with GLCM texture extraction. The integration of GLCM texture extraction with ensemble learning aimed to enhance the accuracy of the model for identifying lung cancer in CT images. The research highlighted the potential for saving millions of lives globally through widespread lung cancer screening programs. Computerized tomography (CT) scans have been a successful imaging modality in medicine for detecting cancer, and in this study, k-means clustering and fuzzy c-means optimization algorithms were applied. The efficiency of the algorithm was assessed, with the fuzzy c-means method achieving the highest precision at 98%. The Gray Level Co-occurrence Matrix (GLCM) was utilized as a crucial tool for feature extraction. Classification techniques such as Support Vector Machine (SVM), Multilayer Perceptron Neural Network (MLPNN), Decision Tree (DT), Logistic Regression, and k-Nearest Neighbors (KNN) were compared against bagging and gradient boosting. Notably, gradient boosting outperformed the others with

an accuracy of 90.9%. The study suggested that utilizing a large dataset could further enhance the precision of the proposed method[5].

Chahade, A. H. et al. conducted a study focusing on medical image feature engineering for the accurate classification of lung and colon cancer types and tissues, with the ultimate goal of contributing to the development of computerized diagnostic systems. The research employed Machine Learning (ML), Information Gain (IG), and Feature Engineering (FE) methods. Various machine learning techniques, including XGBoost, Support Vector Machine (SVM), Random Forest (RF), Linear Discriminant Analysis (LDA), and Multilayer Perceptron (MLP), were applied. Notably, the XGBoost model demonstrated superior performance, achieving a remarkable accuracy of 99% and an F1 score of 98.8%. The authors aspire for their work to become a prominent resource for extracting characteristics crucial for histopathologically precise identification of lung cancer subtypes in the future[6].

Cai, X. et al. employed DeepMeth to achieve early-stage detection of lung cancer in blood samples, presenting a novel strategy for analyzing ctDNA methylation data. The implementation of DeepMeth resulted in a significant improvement, with experiments showing gains of 5–8% relative to the area under the curve (AUC). The study utilized various methods, including Random Forest, XGBoost, LightGBM, Multilayer Perceptron (MLP), Convolutional Neural Network (CNN), and Recurrent Neural Network (RNN). Notably, LightGBM emerged as the top performer, achieving the highest AUC in the evaluations. The potential impact of DeepMeth extends to benefiting liver and breast cancer detection in the near future[7].

Bahatia, S. et al. conducted a study on lung cancer diagnosis using deep learning techniques, particularly focusing on the analysis of CT scans. The research employed various algorithms, including XGBoost and Random Forest. Feature extraction was carried out using UNet and ResNet models. The combination of UNet+Random Forest and ResNet+XGBoost, each individually achieving correctness rates of 74% and 76%, respectively, led to an overall accuracy of 84%. The ensemble of XGBoost and Random Forest classifiers yielded the highest accuracy at 84%[8].

Yakar, M. et al. presented a study on predicting pneumonitis after radiation treatment for Stage III lung cancer using machine learning techniques. The research identified patient and tumor features, dosimetric parameters, and treatment characteristics as risk factors for the development of radiation pneumonitis (RP). Recognizing that RP cannot be attributed to a single parameter, the study aimed to estimate RP growth by applying various machine learning algorithms. The algorithms included Artificial Neural Networks, eXtreme Gradient Boosting (XGB), Logistic Regression, Support Vector Machines, Random Forests, Gaussian Naive Bayes, and Naive Bayes. Notably, the Light Gradient Boosting Machine (LGBM) algorithm emerged as the most effective for predicting RP, achieving a success rate of 85%, a sensitivity of 97%, and a specificity of 50%. The authors suggested that further improvements in accuracy could be attained by employing the LGBM algorithm with more detailed data sheets[9].

Sujitha, R. et al. conducted a study focusing on the classification of lung cancer stages utilizing machine learning within the framework of big data healthcare. Acknowledging the swift accumulation of big data health frameworks and the potential for accurate predictions in early lung cancer detection, the paper emphasized the advantages offered by machine learning. The study provided algorithmic justifications for machine learning within the Apache Spark architecture, designed for the effective classification of lung cancer images and stages. Binary classification involved employing Support Vector Machines (SVM), specifically nonlinear SVM with radial basis function (RBF), and multi-class classification using a threshold method with vector machines. The model aimed at classifying nodules as malignant or benign and determining their malignancy. The highest accuracy achieved by this model was 86%, with other metrics such as an AUC of 0.88. The authors suggested that incorporating a larger dataset could further enhance the accuracy of the model[10].

2.3 Comparative Analysis and Summary

Since then, We've researched the potential uses of lung histopathological images for the diagnosis of other illnesses, such as lung cancer. We thus looked at a few of the research papers written by academics who had previously used histopathological image of the lung to explore similar illnesses.

The given table below shows the comparison of the gained accuracy with other studies and this study.

TABLE 2.3: COMPARISON BETWEEN OTHER STUDIES

Authors	Best Model	Accuracy
Guo, Y.et.al [2021]	com_radNet	74.7%
Althubiti.et.al [2022]	Gradient boosting	90.9%
Mhaske, D. et.al [2021]	GoogLeNet DNN	94.38%
Masud, M.et.al [2021]	Customize CNN	96.33%

2.4 Scope of the problem

The scope of the problem lies in the limitations of existing research studies, characterized by a narrow focus on single illnesses, hindering a comprehensive understanding of medical complexities and restricting the generalizability of findings. Additionally, the scarcity of datasets covering a wide range of disorders poses a challenge, limiting researchers' capacity to conduct thorough studies and impeding the development of robust models for complex medical scenarios.

2.5 Challenges

As researchers, our challenges arose from the disappointment in existing studies not meeting our goals. The predominant focus on single illnesses and the scarcity of diverse datasets for disorders prompted hurdles in classifying three forms of lung cancer from histopathological images. Fine-tuning six Deep Transfer Learning models and eliminating two colon cancer classes were necessary steps to overcome these challenges, ultimately leading to the successful achievement of an unexpectedly high degree of accuracy.

CHAPTER 3

METHODOLOGY

3.1 Research Subject and Instrumentation

The subject of this research is A Comparative Study of Lung Cancer Detection Using Deep Transfer Learning With Keras Tuner. For doing this research, I used Anaconda Prompt, jupyter notebook for programming.

3.2 Data Collection Procedure/Dataset Utilized

The dataset is collected from kaggle. It is a famous dataset, and a lot of work has been done on it already. The dataset comprises 25,000 histopathological images categorized into 5 classes. All images are of dimensions 768 x 768 pixels and are saved in the jpeg file format. This dataset contains two folders named colon image set and lung image set.

For the purpose of detecting only lung cancer, colon set has been deleted. In the lung set, there are three classes: lung adenocarcinoma, lung squamous cell carcinoma and lung benign tissue. Every class contains 5000 images each.

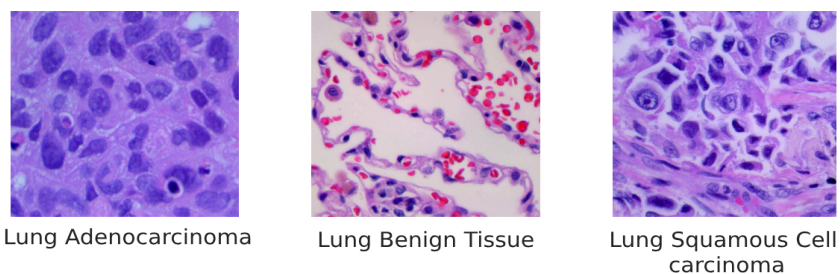


Figure 3.2: Sample Data

Then the dataset has labeled as Train, Test, Validation. The training set comprises 70% of the data, the test set consists of 20%, and the validation set includes 10% of the total data.

TABLE 3.2: DATA DESCRIPTION

Feature	Train70%	Test20%	Validation10%
Lung Adenocarcinoma	3500	1000	500
Lung Squamous Cell Carcinoma	3500	1000	500
Lung Benign Tissue	3500	1000	500
Total	10500	3000	1500

3.3 Statistical Analysis

In our study, we leveraged six pre-trained models, including MobileNetV2, ResNet50, InceptionV3, VGG16, VGG19, and NASNetMobile, for the analysis of image data. Hyperparameter tuning was conducted using Keras Tuner, optimizing key parameters such as learning rates, batch sizes, and optimizers to enhance the performance of the models. This approach allowed us to systematically refine the architecture and parameters for each pre-trained model, contributing to the overall success of our Deep Transfer Learning methodology.

3.3.1 Data Preprocessing

The original pixel values of a picture usually fall between 0 and 255. To expedite and enhance the training process of the neural network, We standardized these values by dividing them by 255, which gave us a rescaled range between 0 and 1. Modifying data for making it usable for a specific task is called preprocessing. In this study we have normalized the pixel values for speeding up the training process, with that we also use augmentations: “Shear Range, Zoom Range and Horizontal Flip.” The batch size was configured as 32, and the input shape was defined as 224x224.

3.3.2 Deep Transfer Learning Architecture

Machine learning encompasses deep learning as a subset, inspired by the structure of the human brain. Deep learning has gained widespread adoption, showcasing remarkable advancements across various industries, particularly in medical image processing. Applying deep learning techniques in healthcare facilitates the extraction of valuable insights and patterns from medical data. Industries in medical sciences leverage deep learning for tasks such as data classification, lesion identification, and data segmentation. Deep learning, especially in image processing, streamlines the classification of medical images like CXR, CT scans, and MRI reports. This has significantly improved the effectiveness of diagnosing critical diseases such as lung cancer, diabetes, skin conditions, and brain tumors. Deep learning research spans multiple domains, with Convolutional Neural Networks (CNN) addressing image processing challenges within the broader category of Deep Neural Networks (DNN). In CNN, visual data input is recognized by computers, converted into a manageable matrix format, and categorized based on distinct visual

patterns. The model learns and creates labels for input images during training, enabling accurate predictions for test images across different categories. CNN primarily employs three layers: the convolutional layer, the pooling layer, and the fully connected layer, enhancing its ability to analyze and predict images effectively.

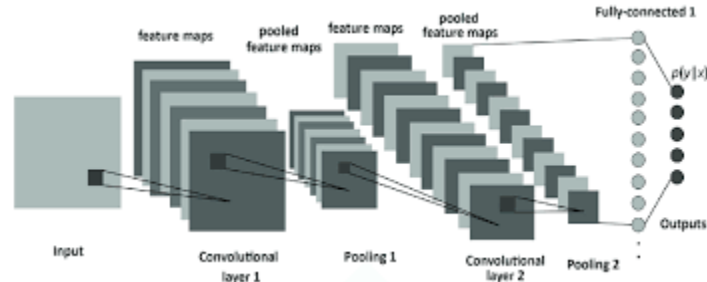


Figure 3.3.2: Transfer Learning Architecture [12]

3.3.3 Convolutional Layer

The initial layer in the sequence of three layers is the Convolutional Layer, serving as the cornerstone in CNN models. This layer is fundamental for processing visual data patterns, involving the filtration of the input image. The filtering process yields a map of function values, shaped by specific kernels applied in the layer. These kernels, employing matrices such as 5x5 and 3x3 transformation matrices, effectively extract both high-level and low-level features from the image data. Utilizing the Stride parameter, the filter compresses images, inducing a changing motion in the image during the CNN process.

$$x_j^l = f\left(\sum_{a=1}^N w_j^{l-1} * y_a^{l-1} + b_j^l\right)$$

In this context, " y_a " represents the a-th feature map of the layer, and " x_j " signifies the j-th feature map of the layer. The notation " w_j " corresponds to the j-th kernel, and " b_j " represents the bias associated with the j-th feature map. The convolution operation is denoted by (*), and N stands for the overall number of features within the layer.

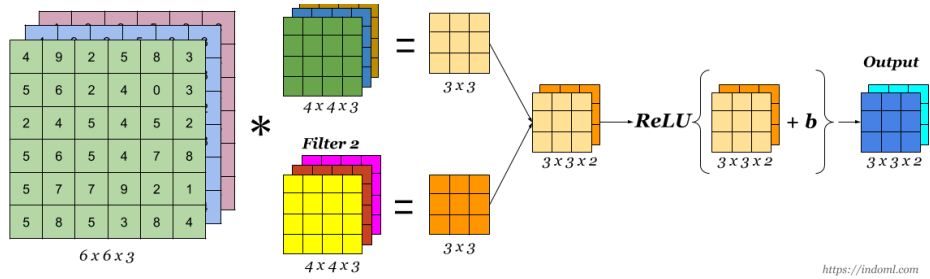


Figure 3.3.3: Convolutional Layer [13]

3.3.4 Pooling Layer

Subsequently, the Pooling layer follows in the sequence. This layer serves to reduce the number of feature maps, enhance computational efficiency, and generate new feature maps. While CNN incorporates multiple pooling layers, our focus here is on two types: maximum pooling and global average pooling. The maximum pooling layer reduces output neurons by creating a new feature map through the maximum values in the image matrix. Following this, the global average pooling layer is employed, weakening the data signal within the matrix. An additional layer introduced to prevent overfitting and network divergence is the dropout layer, strategically placed after the completion of the pooling layer stage.

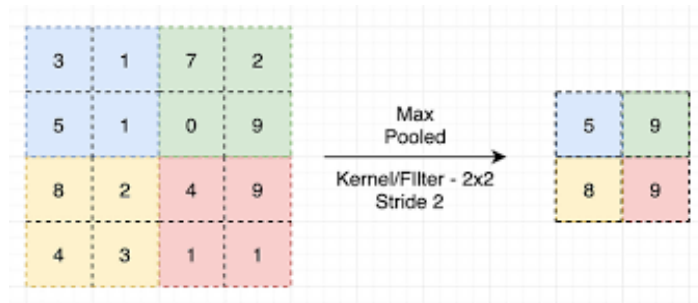


Figure 3.3.4: Pooling Layer [14]

3.3.5 Fully Connected Layer

The ultimate and pivotal layer in CNN is the fully connected layer, employing multilayer backpropagation. This layer serves dual purposes: one for output prediction and the other for fully connecting all features. The fully connected layer incorporates two activation

functions—Rectified Linear Unit (ReLU) and Softmax—to predict the output image. The formulas for these activation functions are illustrated in the equations below.

$$\text{ReLU } f(x) = \max(0,x)$$

$$\text{softmax}(z_j) = \frac{e^{z_j}}{\sum_{k=1}^K e^{z_k}} \text{ for } j = 1, \dots, K$$

Here, "xi" denotes the input data, while "m" represents the number of classes.

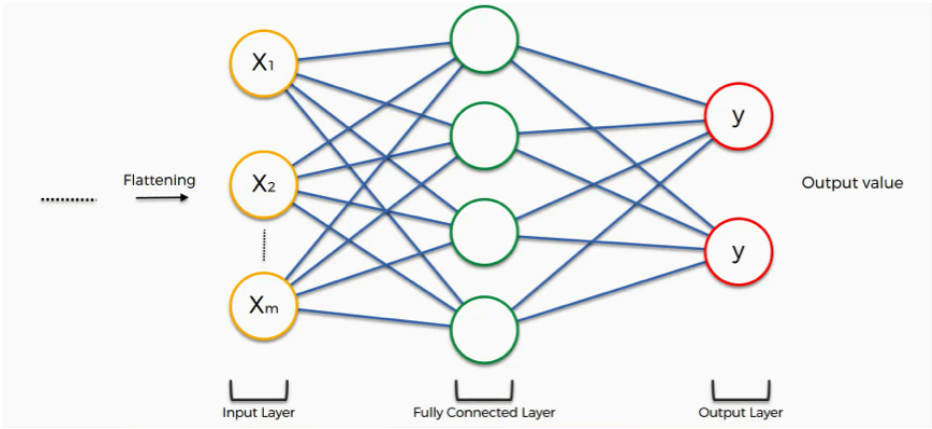


Figure 3.3.5: Fully Connected Layer [15]

3.3.6 Pre-Trained Models

Our project focuses on the early detection of lung cancer, a task often demanding significant amounts of data for effective deep learning. However, manually classifying such datasets by specialists is not only time-consuming but also expensive. Transfer learning emerges as a viable solution, offering a more cost-effective approach to computations and allowing for training on a smaller dataset. Leveraging pre-trained models, such as ResNet50, NASHNetMobile, VGG16, VGG19, InceptionV3, and MobileNetV2, which have been initially trained on extensive datasets like ImageNet, facilitates the transfer of knowledge to our algorithm. This strategy addresses the

challenges posed by limited data and training time. Our application of transfer learning is particularly beneficial for predicting common lung diseases using deep CNN-based models.

3.3.6.1 MobileNetV2

MobileNet-v2 is a convolutional neural network boasting a depth of 53 layers. Its pre-trained configuration enables the classification of images into 1000 object categories, encompassing items like keyboards, mice, pencils, and various animals. Designed to excel on mobile devices, MobileNetV2 serves as a highly efficient feature extractor for tasks such as object detection and segmentation. When coupled with the recently introduced SSDLite, the updated model demonstrates a remarkable 35% increase in speed while maintaining the same level of accuracy compared to its predecessor, MobileNetV1. MobileNetV2 is the cutting-edge object identification algorithm to find the face mask in real-time. The proposed method efficiently handles object detection and contributes to high object detection accuracy of 99.6 percent and decreased object detection time.

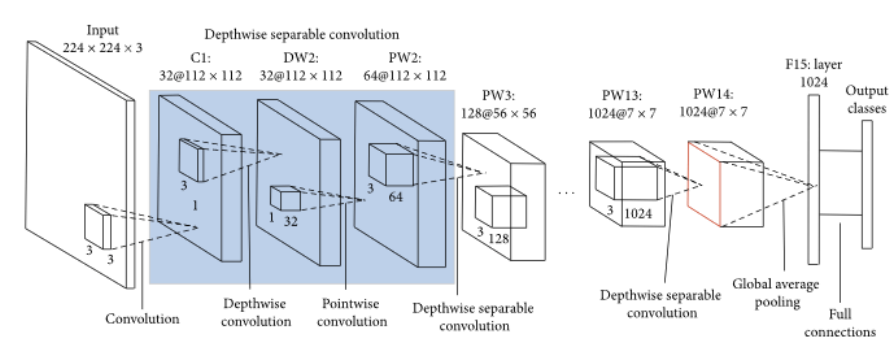


Figure 3.3.6.1: Architecture of MobileNetV2 [16]

Below, the given image shows the working architecture of MobileNetV2 with customized layers.

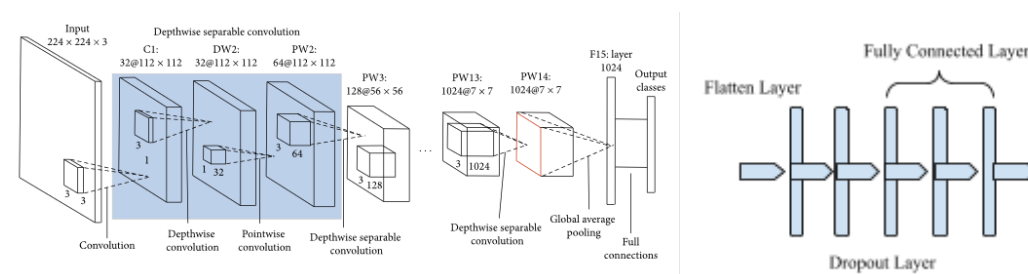


Figure 3.3.6.2: MobileNetV2 with Customized Layers

3.3.6.2 ResNet50

ResNet-50, a convolutional neural network with a depth of 50 layers, derives its name from "Residual Network." It represents a specific category of convolutional neural networks (CNN) introduced in the 2015 paper titled "Deep Residual Learning for Image Recognition." ResNet addresses the challenge of the "vanishing gradient" problem commonly encountered in deep networks, enabling the construction of networks with potentially thousands of convolutional layers that surpass the performance of shallower counterparts. A key advantage lies in its capacity to effectively train extremely deep networks, achieved through the incorporation of residual blocks and skip connections, facilitating the retention of information from earlier layers. This innovative neural network is specifically designed for image classification tasks.

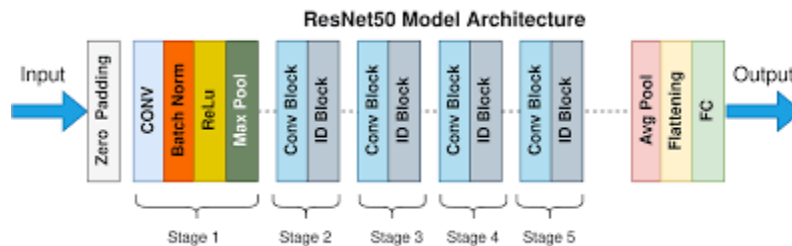


Figure 3.3.6.3: Architecture of ResNet50 [17]

3.3.6.3 Inception V3

Inception v3, an image recognition model, has demonstrated an accuracy exceeding 78.1% on the ImageNet dataset. Represented as a convolutional neural network with a depth of 48 layers, Inception v3 follows the model architecture outlined in the paper "Rethinking the Inception Architecture for Computer Vision." Notably, the inception_v3 requires a minimum input size of 75x75. It's crucial to highlight that, unlike other models, inception_v3 expects tensors sized $N \times 3 \times 299 \times 299$. Therefore, it's imperative to resize images accordingly. Inception v3 incorporates transfer learning as a popular technique for image classification. This approach involves reusing a pre-trained model on a new task, leveraging a small dataset to enhance performance and reduce training time.

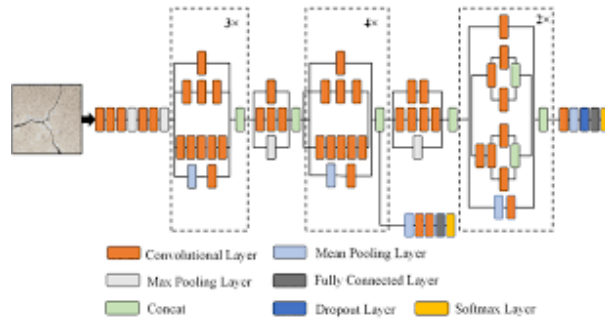


Figure 3.3.6.4: Architecture of InceptionV3 [18]

3.3.6.4 VGG16

VGG16, recognized as the top-performing model on the ImageNet dataset, has played a pivotal role in advancing computer vision. In the pursuit of empowering computers to comprehend visual information, VGG16 stands out as a crucial milestone, marking a significant breakthrough. Its success has not only contributed to the field of image recognition but has also paved the way for subsequent advancements and achievements in the domain.

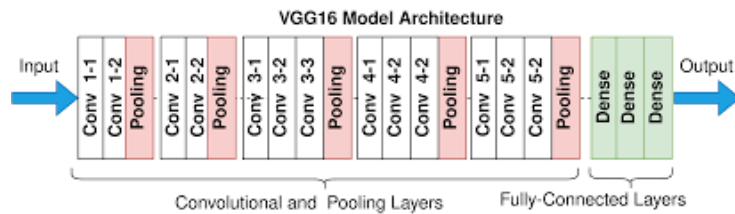


Figure 3.3.6.5: Architecture of VGG16 [19]

3.3.6.5 VGG19

VGG19 is a specific variant within the VGG model family, characterized by 19 layers, including 16 convolution layers, 3 fully connected layers, 5 MaxPool layers, and 1 SoftMax layer. The architecture of this network is designed to receive input in the form of a fixed-size RGB image with dimensions 224 by 224 pixels, implying a structured matrix of (224, 224, 3).

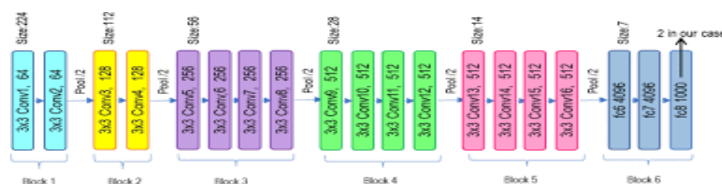


Figure 3.3.6.6: Architecture of VGG19 [20]

3.3.6.6 NASNetMobile

NASNet, short for Neural Architecture Search Network dedicated to image classification, operates with an image input size of 331 by 331 pixels. Representing a machine learning model, NASNet, which stands for Neural Architecture Search Network, demonstrates notable performance. Evaluation of the model indicates an accuracy of 93.20% when using RGB images and 83.60% with grayscale images. The model has a size of 15.54 megabytes and comprises 4.28 million parameters.

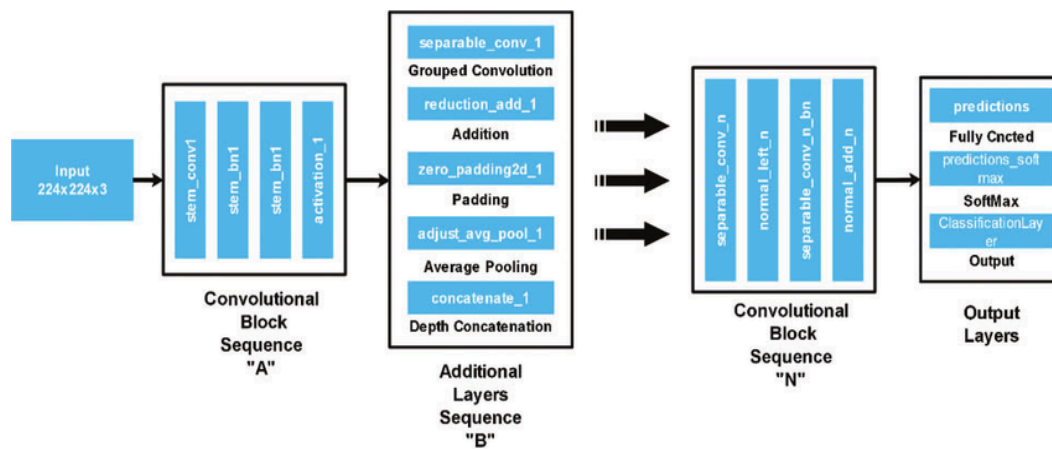


Figure 3.3.6.7: Architecture of NASNetMobile [21]

3.3.7 Model Tuning and Model Training

Essentially, tuning entails adjusting a set of hyperparameters through a trial-and-error process. Checking the accuracy and performance of the model every time for a specific parameter and then changing it is very time consuming.

The most crucial part is the training part which takes the most time. Keras Tuner solve the problem of tuning hyper parameter every time manually. With a process of random search, and a set of trails, keras tuner at first search for the best parameter and then put them into the model for training, then again it searches for another set of parameters and train the model. In our project, we set the trail for 5 time. After completing these trails, the best parameter got save with a name of best_model then it evaluates the test set.

The figure below given shows the workflow of keras tuner.

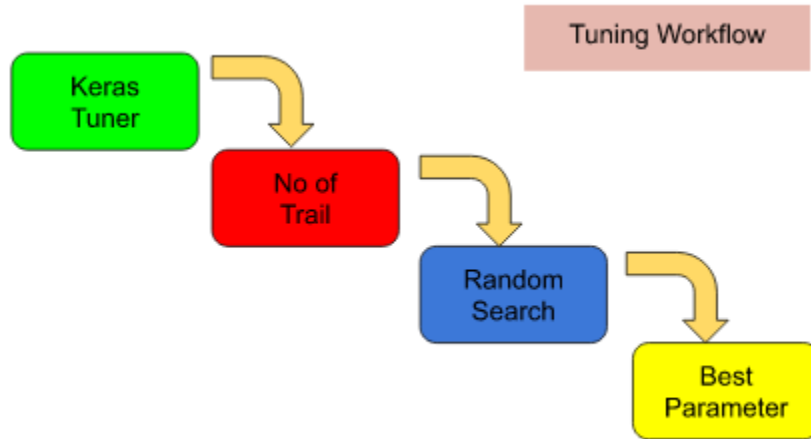


Figure 3.3.7: WorkFlow of Keras Tuner

For our study, we divided the dataset into three part as train, test and validation. Train part contain 70% of data, test part contains 20 and validation part contain 10% data.

The model is trained using the Adam optimizer in conjunction with categorical cross-entropy. Evaluation is performed on the validation set after each epoch.

3.3.8 Parameter Optimization

Throughout the simulation, we concentrated on a few aspects of our proposed model to increase its effectiveness. The batch size was increased from sixteen to thirty-two. It enhanced ours model's performance. 10 epochs were thus employed. In the instance of the activation function, we used "ReLU" and "Softmax" as classification algorithms. Both algorithms are activation functions. reducing loss of training. For tuning hyper parameter, we employed keras tuner. It randomly searches for 5 trail for the best parameter and then set these values in the best_model. Every trail takes 10 epochs thus the total number of epochs was 60 for this task. This is how the best parameter has been found for this disease detection study.

3.4 Proposed Methodology/Applied Mechanism

The figure shows below is the proposed methodology of this study.

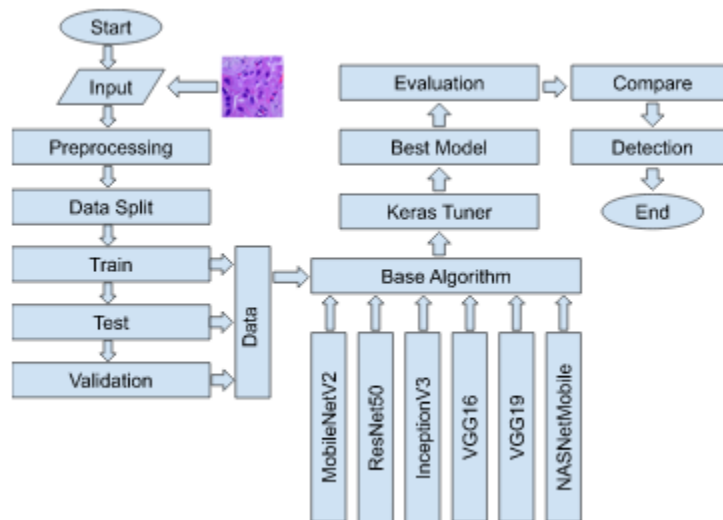


Figure 3.4: Workflow of the Proposed Methodology

This proposed model of us has some stages of workflow including preprocessing of data, data split, applying pre-trained models, adding keras tuner for parameter tuning and finding the best model, performance evaluation, performance compare and then disease detection.

- **Preprocessing:** As the original pixel values of an image contains value typically in a range of 0 to 255. For stabilizing and accelerating the training process of neural network, we normalized these values by dividing it with 255. By doing this we got a re-scaled range between 0 and 1.
- **Data Splitting:** For the training of the model that we have built, The dataset has been segmented into three groups: Training, Testing, and Validation. Train sector got 70% of the total data, test sector got 20% and the validation sector got 10% of the total data.
- **Pre-Trained Algorithms:** In this stage, six pre-trained algorithms were used for feature extraction. With these pre-trained weights we employed some custom layers for the processing of the transfer learning model.
- **Keras Tuner:** In this transfer learning model, keras tuner got the main role for finding out the best hyperparameter for the custom layers that we have employed. For this study,

we set the max trial value 5 as the tuner will random search for the best parameter for 5 times and then it will save all the tuned values.

- **Best Model:** After the trial has done for 5 times, in this stage a model will automatically be created with the best found hyperparameter for the final training period.
- **Performance Evaluation:** In this section, all the data is visualized through graphs. Accuracy and loss graphs for both training and validation phases are presented post the training and testing processes. Given the utilization of six models in this study, six confusion matrices illustrate the count of conflicting data. Additionally, measures such as precision, f1-score, and recall are showcased in this implementation.
- In the concluding segment, we summarized our findings and outlined plans for future research..

3.5 Implementation requirements

In our image classification study, we utilized pre-trained models for analysis, incorporating essential tools such as Keras Tuner, TensorFlow, Image Data Generator, and Jupyter Notebook. The implementation was supported by a dedicated GPU, specifically the GeForce RTX 2060, to enhance computational efficiency.

CHAPTER 4

EXPERIMENTAL RESULTS & DISCUSSION

4.1 Experimental Setup

Our implementation is conducted on a Windows 10 laptop equipped with an 8th generation Intel(R) Core(TM) i5-8265U CPU operating at 1.60GHz and 1.80GHz, with a total of 20 GB RAM. The execution of the model takes place within a Jupyter notebook environment, utilizing the Keras and Tensorflow frameworks.

4.2 Experimental Result and Analysis

We built our own neural network using the transfer learning approach and the Keras tuner for parameter tuning. We put up six distinct transfer learning designs. such as MobileNetV2, ResNet50, NASHNetMobile, InceptionV3, VGG-16, and VGG-19.

A comparison of the final training and testing accuracy of multiple models is shown in Table 4.2.1.

TABLE 4.2.1: COMPARISON OF THIS STUDY

Pre-trained Models	Train Accuracy	Test Accuracy
MobileNetV2	98.26	98.47
InceptionV3	96.89	97.27
ResNet50	78.95	82.87
VGG16	97.18	98.40
VGG19	97.39	98.37
NASHNetMobile	96.65	97.23

For MobileNetV2 Model:

In this context, MobileNetV2 surpasses all other models, achieving an outstanding accuracy of 98.47%. The graphical representation of Training-Validation Accuracy and Training-Validation Loss for MobileNetV2 is depicted in Figure 4.2.1. The first section illustrates Train Accuracy and Validation Accuracy, while the second section portrays Training Loss and Validation Loss. The blue line represents training loss and accuracy, while the orange line represents validation loss and accuracy.

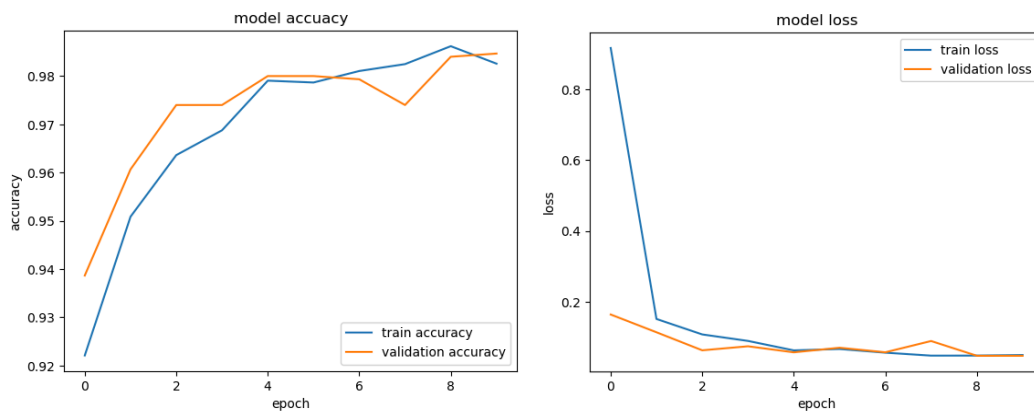


Figure 4.2.1: MobileNetV2 Training-Validation Loss and Accuracy.

When an algorithm encounters conflicting data, it results in an error. Despite being selected as the most suitable model for my research, this model still experiences errors attributed to technological constraints. When tasked with diagnosing an illness or categorizing multiple classes, the machine may encounter confusion.

In this instance, Figure 4.2.2 illustrates a total of 46 instances of data conflicts. Within the Lung_aca class, there are 12 conflicts with the Lung_scc class and no conflicts with the Lung_n class. The Lung_n class encounters 3 data conflicts with the Lung_aca class and none with the Lung_scc class. As for the Lung_scc class, it experiences 31 data conflicts with the Lung_aca class and none with the Lung_n class.

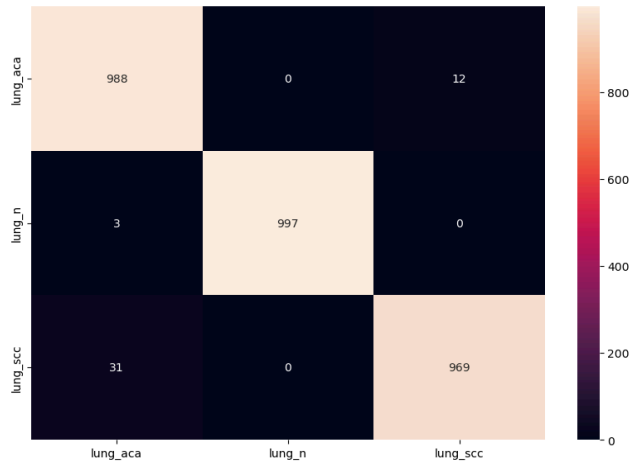


Figure 4.2.2: Confusion Matrix of MobileNetV2.

The following values indicate precision, recall, f1-score, and support for the MobileNetV2 model.

TABLE 4.2.2: CLASSIFICATION REPORT OF MOBILENETV2

Feature	Precision	Recall	F1-Score	Support
Lung_aca	0.97	0.99	0.98	1000
Lung_n	1.00	1.00	1.00	1000
Lung_scc	0.99	0.97	0.98	1000

For ResNet50 Model:

In this case, the graphical representation in Figure 4.2.3 illustrates the training-validation accuracy and training-validation loss of ResNet50. The first section showcases Train & Validation Accuracy, while the second section displays Training Loss & Validation Loss. The blue line represents training loss and accuracy, whereas the orange line indicates validation loss and accuracy.

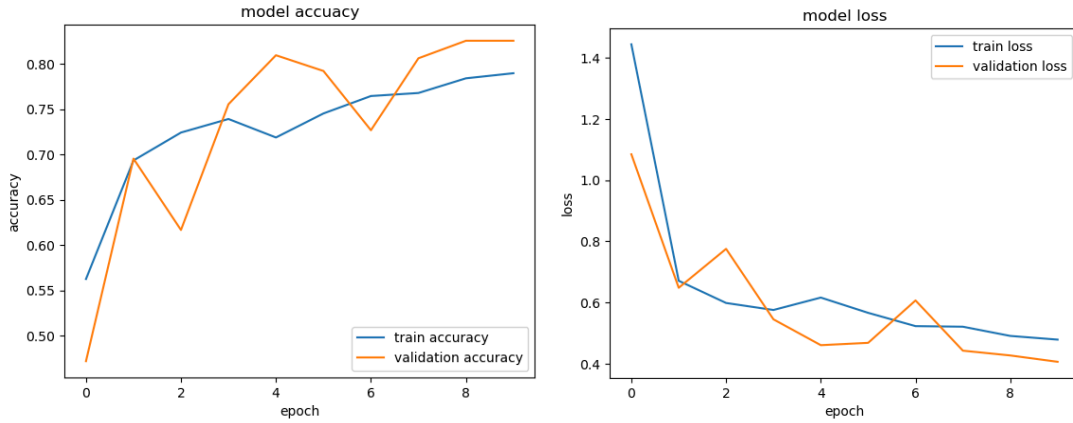


Figure 4.2.3: ResNet50 Training-Validation Loss and Accuracy.

In this context, Figure 4.2.4 illustrates a total of 514 instances of data conflicts. Here, we can see that Lung_aca class has 75 data conflicts with Lung_n and 183 data conflicts with Lung_scc class. Lung_n class has 21 data conflicts with Lung_aca and zero conflicts with Lung_scc class. Lung_scc class has 229 data conflicts with Lung_aca class and 6 data conflicts with Lung_n class.

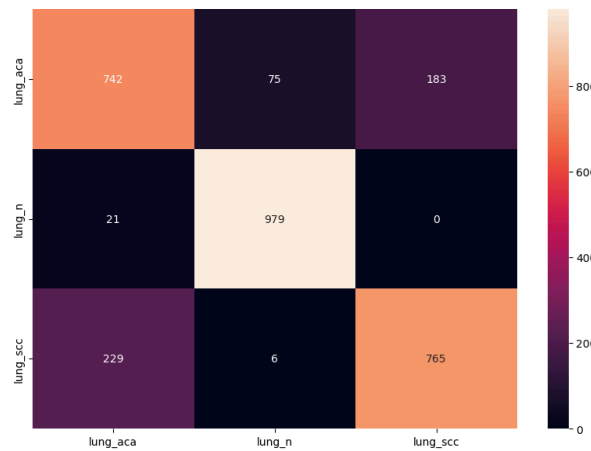


Figure 4.2.4: Confusion Matrix of ResNet50.

The following values depict precision, recall, f1-score, and support for the ResNet50 model.

TABLE 4.2.3: CLASSIFICATION REPORT OF RESNET50

Feature	Precision	Recall	F1-Score	Support
Lung_aca	0.75	0.74	0.74	1000
Lung_n	0.92	0.98	0.95	1000
Lung_scc	0.81	0.77	0.79	1000

For InceptionV3 Model:

In this case, the performance metrics, specifically the training-validation accuracy and training-validation loss of InceptionV3, are visualized through a graph represented in Figure 4.2.5. The graph is designed to illustrate the Train & Validation Accuracy in the initial segment, denoting the training accuracy and validation accuracy. The second segment focuses on Training Loss & Validation Loss. The graph incorporates a blue line to represent training loss and accuracy, while an orange line is utilized to depict validation loss and accuracy.

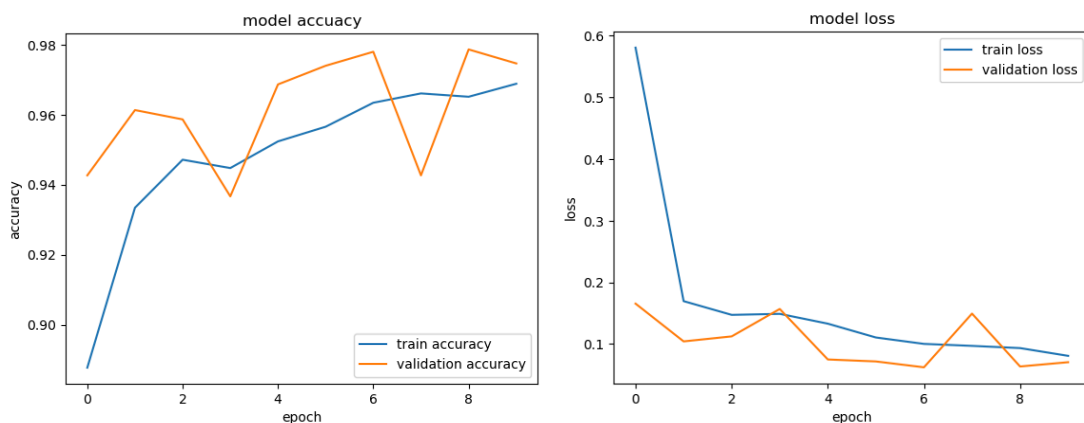


Figure 4.2.5: InceptionV3 Training-Validation Loss and Accuracy.

In this context, Figure 4.2.6 illustrates a cumulative count of 82 instances of data conflicts. Here, we can see that Lung_aca class has 17 data conflicts with Lung_n and 49 data conflicts with

Lung_scc class. Lung_n class has 0 data conflicts with Lung_aca and zero conflicts with Lung_scc class. Lung_scc class has 16 data conflicts with Lung_aca class and 0 data conflicts with Lung_n class.

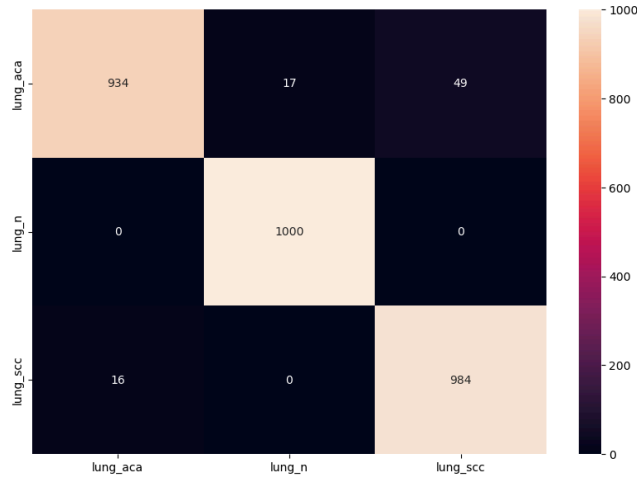


Figure 4.2.6: Confusion Matrix of InceptionV3.

The precision, recall, f1-score, and support metrics for the InceptionV3 model are presented here.

TABLE 4.2.4: CLASSIFICATION REPORT OF INCEPTIONV3

Feature	Precision	Recall	F1-Score	Support
Lung_aca	0.98	0.93	0.96	1000
Lung_n	0.98	1.00	0.99	1000
Lung_scc	0.95	0.98	0.97	1000

For VGG16 Model:

In this case, the graph in Figure 4.2.7 illustrates the training-validation accuracy and training-validation loss for the VGG16 model. The graph is designed to depict Train & Validation Accuracy in the initial section, representing Training Loss & Validation Loss in the

subsequent part. The blue line corresponds to training loss and accuracy, while the orange line signifies validation loss and accuracy.

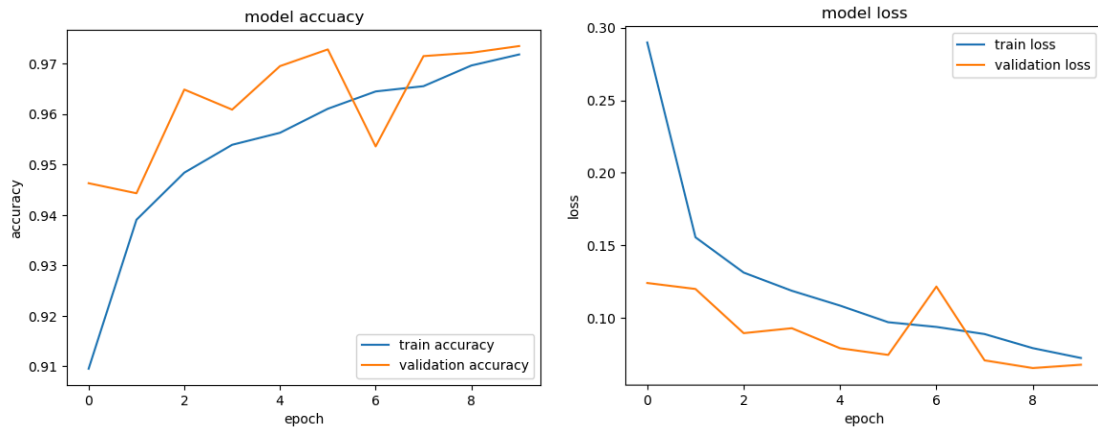


Figure 4.2.7: VGG16 Training-Validation Loss and Accuracy.

In this context, Figure 4.2.8 displays a cumulative count of 48 instances of data conflicts. Specifically, within the Lung_aca class, there are no conflicts with the Lung_n class and 12 conflicts with the Lung_scc class. The Lung_n class exhibits 1 conflict with the Lung_aca class and none with the Lung_scc class. Meanwhile, the Lung_scc class shows 35 conflicts with the Lung_aca class and none with the Lung_n class.

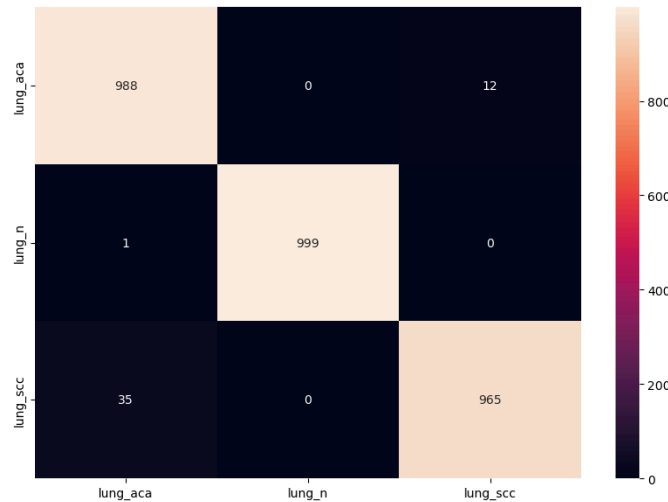


Figure 4.2.8: Confusion Matrix of VGG16.

For the VGG16 model, the precision, recall, f1-score and support are shown below.

TABLE 4.2.5: CLASSIFICATION REPORT OF VGG16

Feature	Precision	Recall	F1-Score	Support
Lung_aca	0.96	0.99	0.98	1000
Lung_n	1.00	1.00	1.00	1000
Lung_scc	0.99	0.96	0.98	1000

For VGG19 Model:

In this case, the graphical representation in Figure 4.2.9 depicts the training-validation accuracy and training-validation loss of VGG19. The first section illustrates Train & Validation Accuracy, while the second section presents Training Loss & Validation Loss. The blue line represents training loss and accuracy, while the orange line indicates validation loss and accuracy.

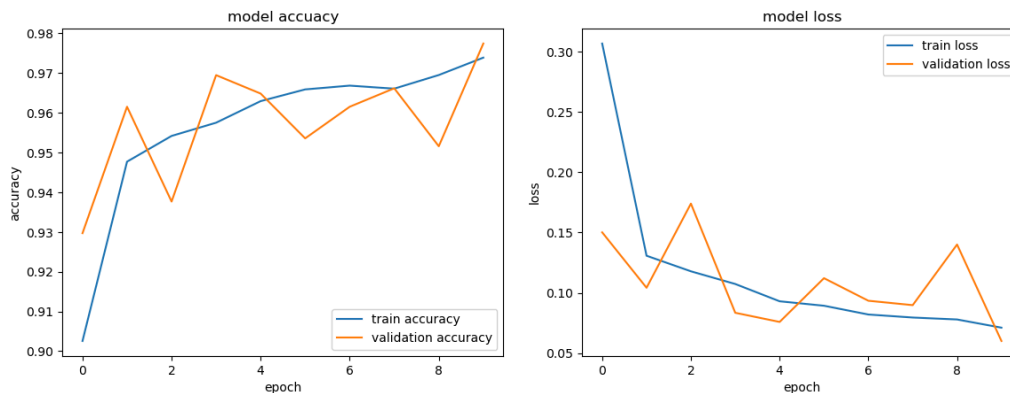


Figure 4.2.9: VGG19 Training-Validation Loss and Accuracy.

In this context, Figure 4.2.10 illustrates a total of 49 instances of data conflicts. From the given figure we can illustrate that Lung_aca class has 0 data conflicts with Lung_n class and 35 data conflicts with Lung_scc class. Lung_n class has 4 data conflicts with Lung_n class and zero data

conflicts with Lung_scc class. Lung_scc class has 10 data conflicts with Lung_aca class and 0 data conflicts with Lung_n class.

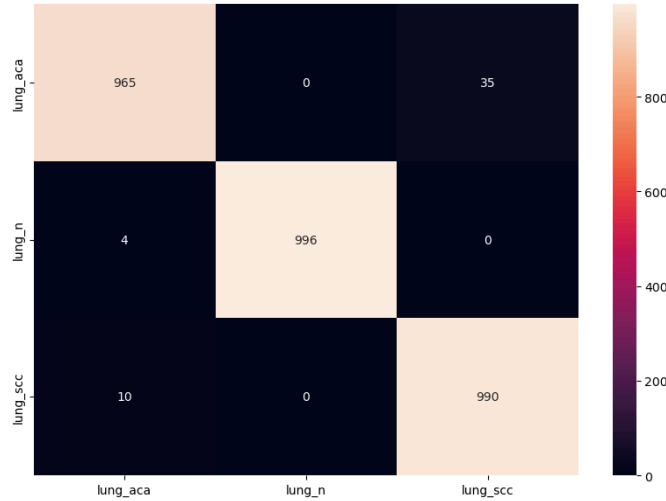


Figure 4.2.10: Confusion Matrix of VGG19.

The precision, recall, f1-score, and support for the VGG19 model are presented below.

TABLE 4.2.6: CLASSIFICATION REPORT OF VGG19

Feature	Precision	Recall	F1-Score	Support
Lung_aca	0.99	0.96	0.98	1000
Lung_n	1.00	1.00	1.00	1000
Lung_scc	0.97	0.99	0.98	1000

For NASHNetMobile Model:

In this case, the graphical representation in Figure 4.2.11 illustrates the training-validation accuracy and training-validation loss of NASHNetMobile. The first section showcases Train & Validation Accuracy, while the second section displays Training Loss & Validation Loss. The

blue line represents training loss and accuracy, whereas the orange line indicates validation loss and accuracy.

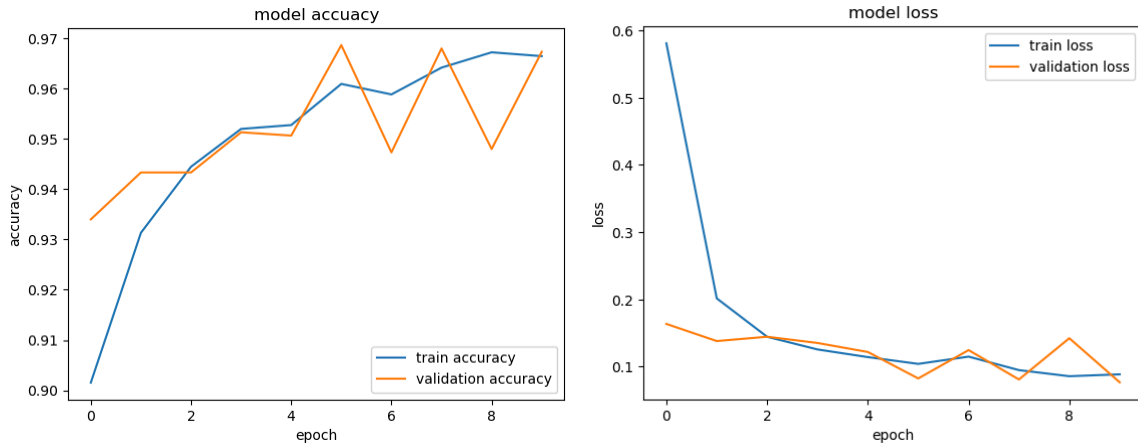


Figure 4.2.11: NASHNetMobile Training-Validation Loss and Accuracy.

In this instance, Figure 4.2.12 displays a total of 83 instances of data conflicts. We can see that the Lung_aca class 1 data conflicts with Lung_n class and 67 data conflicts with Lung_scc class. Lung_n class has 0 data conflicts with both Lung_aca and Lung_scc class. Lung_scc class has 15 data conflicts with Lung_aca class and 0 data conflicts with Lung_n class.

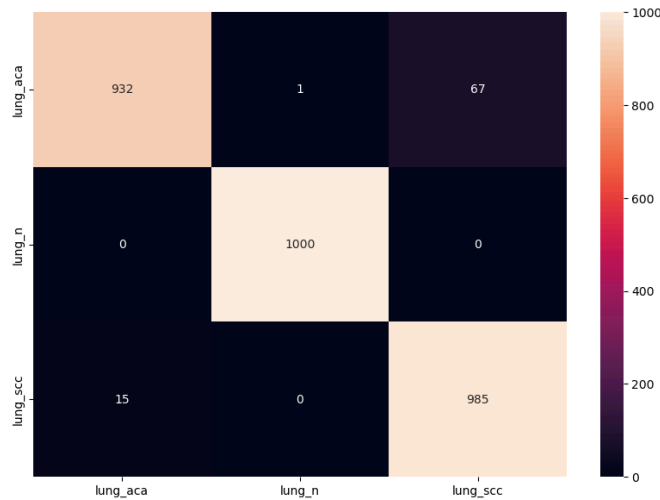


Figure 4.2.12: Confusion Matrix of NASHNetMobile.

The precision, recall, f1-score, and support for the NASHNetMobile model are presented below.

TABLE 4.2.7: CLASSIFICATION REPORT OF NASHNETMOBILE

Feature	Precision	Recall	F1-Score	Support
Lung_aca	0.98	0.93	0.96	1000
Lung_n	1.00	1.00	1.00	1000
Lung_scc	0.94	0.98	0.96	1000

4.3 Discussion

Throughout this study we have observed that after tuning hyperparameters we got the best accuracy. We have studied many other research papers on this domain and they also did great work finding out the category of lung disease. As discussed previously, the dataset was collected from online resources. It had five classes, two of them were for colon cancer and three were lung cancers. For detecting only the category of lung cancer, we have dropped two classes of colon cancer, and then we have splitted the datasets class into three category: Train, Test and Validation. Train part contains the most of the data 70%, Test part got 20% and Validation part got 10% of the data from the three classes of lung cancer.

From our study of other papers, no one has used keras tuner for parameter tuning, thus we employed keras tuner with transfer learning model that tune the neuron of our custom layers and set the best possible values for neurons and also the dropout rate. The model searches for five trails and then it saves the best parameter thus we found the best model.

CHAPTER 5

IMPACT ON SOCIETY, ENVIRONMENT & SUSTAINABILITY

5.1 Impact on Society

The impact of lung cancer detection on society includes improvements in medical sector, economic growth, sustainable medical practices, enhanced consumer satisfaction, less waste of time. All of these beneficial effects add to the health of people, communities, and the environment.

5.2 Impact on Environment

Lung cancer detection's positive impact on the environment lies in promoting sustainable medical sector practices, reducing human efforts, minimizing cost. These initiatives help make the medical field more sustainable and ecologically friendly while advancing early lung cancer detection.

5.3 Ethical Aspects

Fair treatment, market openness, customer trust and safety, sustainable methods, worker welfare, social and economic impact, and refraining from dishonest activities are all considered ethical aspects of lung cancer classification. The medical industry can benefit consumers and the industry by promoting sustainability, fairness, and openness throughout the supply chain by upholding ethical standards.

5.4 Sustainability Plan

A comprehensive sustainability plan for lung cancer classification can help the medical field promote social cohesion, economic resilience, and environmental preservation. It solves the ethical and sustainability issues related to illness detection, promotes customer trust, and supports the long-term viability of disease detection.

CHAPTER 6

SUMMARY, CONCLUSION, RECOMMENDATION AND IMPLICATION FOR FUTURE RESEARCH

6.1 Summary of the Study

This study aims to build a robust model for classifying lung cancer using a medium-sized dataset of 15,000 images divided into three classes. Leveraging histopathological images and deep transfer learning, particularly with Keras Tuner, the research successfully identifies cancer types automatically. Among various transfer learning models, MobileNetV2 demonstrated the highest accuracy, surpassing previous studies. Training utilized 70% of the data, with 20% for testing and 10% for validation. The findings suggest the effectiveness of deep transfer learning for accurate lung cancer classification on medium-sized datasets.

6.2 Conclusion

The main focus of this work is to build a model that can perform well on a medium level dataset as the dataset contains only 15000 images of lung cancer which is divided into three classes. From the outcome of the model we can see that by utilizing histopathological images of lung cancer, deep transfer learning methods can be used to automatically identify the type of cancer. With the help of keras tuner, this method works well on classifying these diseases as the tuner is automatically finding the best parameter for this classification task. The MobileNetV2 model produced the best accuracy out of all the transfer learning models we have used. For identifying the category of lung cancer, we trained about 70% of data and for testing purpose 20% of data had been used and 10% for validation. By validating multiple models, we found that the MobileNetV2 is giving us the highest accuracy among all other models that we have used and also this performance also beat previous studies.

6.3 Implication for Further Study

In future our target is to select a more large dataset which contains more classes. We will work more on lung cancer detection with a big dataset, For increasing the efficiency we will create a more complex CNN model with keras tuner for parameter tuning that consumes less time and will provide more accurate results. If found a real time dataset then our target is to apply more

preprocessing techniques for preparing that data suitable for performing more transfer learning algorithms with complex CNN customized models. We will create an android application for detecting lung cancer in future. The medical field will benefit greatly from this as it will make diagnosing any lung-related condition much easier.

REFERENCES

- [1] Guo, Y., Song, Q., Jiang, M., Guo, Y., Xu, P., Zhang, Y., ... Yao, X. (2021). Histological subtypes classification of lung cancers on CT images using 3D deep learning and radiomics. *Academic radiology*, 28(9), e258-e266.
- [2] AL-Huseiny, M. S., Sajit, A. S. (2021). Transfer learning with GoogLeNet for detection of lung cancer. *Indonesian Journal of Electrical Engineering and Computer Science*, 22(2), 1078-1086.
- [3] Cai, Z., Xu, D., Zhang, Q., Zhang, J., Ngai, S. M., Shao, J. (2015). Classification of lung cancer using ensemble-based feature selection and machine learning methods. *Molecular BioSystems*, 11(3), 791-800.
- [4] Radhika, P. R., Nair, R. A., Veena, G. (2019, February). A comparative study of lung cancer detection using machine learning algorithms. In *2019 IEEE International Conference on Electrical, Computer and Communication Technologies (ICECCT)* (pp. 1-4). IEEE.
- [5] Althubiti, S. A., Paul, S., Mohanty, R., Mohanty, S. N., Alenezi, F., Polat, K. (2022). Ensemble Learning Framework with GLCM Texture Extraction for Early Detection of Lung Cancer on CT Images. *Computational and Mathematical Methods in Medicine*, 2022.
- [6] Chehade, A. H., Abdallah, N., Marion, J. M., Oueidat, M., Chauvet, P. (2022). Lung and Colon Cancer Classification Using Medical Imaging: A Feature Engineering Approach.
- [7] Cai, X., Tao, J., Wang, S., Wang, Z., Wang, J., Li, M., ... Ji, H. (2022). Noninvasive Lung Cancer Early Detection via Deep Methylation Representation Learning.
- [8] Bhatia, S., Sinha, Y., Goel, L. (2019). Lung cancer detection: a deep learning approach. In *Soft Computing for Problem Solving* (pp. 699-705). Springer, Singapore.
- [9] Yakar, M., Etiz, D., Metintas, M., Ak, G., Celik, O. (2021). Prediction of radiation pneumonitis with machine learning in stage III lung cancer: a pilot study. *Technology in cancer research treatment*, 20, 15330338211016373.
- [10] Sujitha, R., Seenivasagam, V. (2021). Classification of lung cancer stages with machine learning over big data health care framework. *Journal of Ambient Intelligence and Humanized Computing*, 12(5), 5639-5649.
- [11] Masud, M., Sikder, N., Nahid, A. A., Bairagi, A. K., & AlZain, M. A. (2021). A machine learning approach to diagnosing lung and colon cancer using a deep learning-based classification framework. *Sensors*, 21(3), 748.
- [12] IBM, available at <<<https://rb.gy/ewkxv4>>> last accessed on October 22, 07:00 PM.

- [13] Medium, available at <<<https://rb.gy/7tma2b>>> last accessed on October 22, 07:15 PM.
- [14] Medium, available at <<<https://rb.gy/0w8pnl>>> last accessed on October 22, 07:18 PM.
- [15] SuperDataScience, available at <<<https://shorturl.at/bfsA2>>> last accessed on October 22, 07:22 PM.
- [16] WikiDocs, available at <<<https://wikidocs.net/165429>>> last accessed on October 22, 07: 26 PM.
- [17] Medium, available at << <https://towardsdatascience.com/the-annotated-resnet-50-a6c536034758>>> last accessed on October 22, 07:32 PM.
- [18] ResearchGate, available at << <https://shorturl.at/oKQU0>>> last accessed on October 22, 07:39 PM.
- [19] Medium, available at << <https://shorturl.at/nlPQX>>> last accessed on October 23, 10: 12 PM.
- [20] ResearchGate, available at <<<https://shorturl.at/hnp78>>> last accessed October 23, 10:20 PM.
- [21] ResearchGate, available at <<<https://shorturl.at/clCIY>>> last accessed on October 23, 10:27 PM.

ORIGINALITY REPORT

23%

SIMILARITY INDEX

16%

INTERNET SOURCES

13%

PUBLICATIONS

12%

STUDENT PAPERS

PRIMARY SOURCES

1	Submitted to Gazi University Student Paper	9%
2	Rahul Deb Mohalder, Khandkar Asif Hossain, Juliet Polok Sarkar, Laboni Paul, M. Raihan, Kamrul Hasan Talukder. "Chapter 17 Lung Cancer Detection from Histopathological Images Using Deep Learning", Springer Science and Business Media LLC, 2023 Publication	2%
3	dspace.daffodilvarsity.edu.bd:8080 Internet Source	2%
4	repository.tudelft.nl Internet Source	1%
5	ebin.pub Internet Source	1%
6	link.springer.com Internet Source	1%
7	dspace.bracu.ac.bd:8080 Internet Source	1%
